

8-1991

Dihydropyran Ring Conformations. I. Structures of 2-Methoxy- and 2-Hydroxy-2, 4-dimethyl-3, 4-dihydro-2*H*, 5*H*-Pyrano[3,2-*c*][1]benzopyran-5-ones

Edward J. Valente
University of Portland, valentee@up.edu

Drake S. Eggleston

Follow this and additional works at: http://pilot scholars.up.edu/chm_facpubs

 Part of the [Chemistry Commons](#)

Citation: Pilot Scholars Version (Modified MLA Style)

Valente, Edward J. and Eggleston, Drake S., "Dihydropyran Ring Conformations. I. Structures of 2-Methoxy- and 2-Hydroxy-2, 4-dimethyl-3, 4-dihydro-2*H*, 5*H*-Pyrano[3,2-*c*][1]benzopyran-5-ones" (1991). *Chemistry Faculty Publications and Presentations*. 19. http://pilot scholars.up.edu/chm_facpubs/19

This Journal Article is brought to you for free and open access by the Chemistry at Pilot Scholars. It has been accepted for inclusion in Chemistry Faculty Publications and Presentations by an authorized administrator of Pilot Scholars. For more information, please contact library@up.edu.

Dihydropyran Ring Conformations. I. Structures of 2-Methoxy- and 2-Hydroxy-2,4-dimethyl-3,4-dihydro-2*H*,5*H*-pyrano[3,2-*c*][1]benzopyran-5-ones

BY EDWARD J. VALENTE

Department of Chemistry, Mississippi College, Clinton, MS 39058, USA

AND DRAKE S. EGGLESTON

Department of Physical and Structural Chemistry, Smith, Kline and French Laboratories, King of Prussia, PA 19406, USA

(Received 17 July 1990; accepted 2 January 1991)

Abstract

Conformations of embedded 3,4-dihydro-2*H*-pyrans (DHP's) are studied in a closely related series of nine

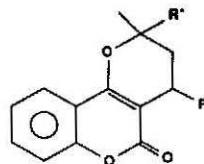
molecular structures, including the *cis* and *trans* isomers of both racemic and resolved homologs of 2,4-dimethyl-3,4-dihydro-2*H*,5*H*-pyrano[3,2-*c*][1]-benzopyran-5-one. DHP rings in these structures

display a range of conformations near the half-chair form but distorted variously toward each of the two inequivalent *d,e*- and *e,f*-diplanar forms. Factor analysis reveals the coordination of torsional motions associated with a principal ring-bending mode based on the various ring conformations. Two methyl ketals and an hemiketal structure are reported. (I): (2*S*,4*S*)-*cis*-2-methoxy, C₁₅H₁₆O₄, *M_r* = 260.30, trigonal, *P*3₂21, *a* = 9.579 (5), *c* = 24.938 (15) Å (hexagonal axes), *V* = 1981.7 (33) Å³, *Z* = 6, *D_x* = 1.309 g cm⁻³, λ(Mo *K*α) = 0.71073 Å, μ = 0.884 cm⁻¹, *F*(000) = 828, *T* = 295 K, *R* = 0.040 for 1470 observations. (II): (2*R*,4*S*)-*trans*-2-methoxy, C₁₅H₁₆O₄, *M_r* = 260.30, monoclinic, *P*2₁, *a* = 9.254 (4), *b* = 11.970 (5), *c* = 12.736 (5) Å, β = 105.64 (4)°, *V* = 1358.5 (22) Å³, *Z* = 4 (two molecules per asymmetric unit), *D_x* = 1.274 g cm⁻³, λ(Mo *K*α) = 0.71073 Å, μ = 0.860 cm⁻¹, *F*(000) = 552, *T* = 295 K, *R* = 0.043 for 2923 observations. (III): (2*S*,4*S*)-*cis*-2-hydroxy, C₁₄H₁₄O₄, *M_r* = 246.27, orthorhombic, *P*2₁2₁2₁, *a* = 6.816 (3), *b* = 12.826 (7), *c* = 13.949 (6) Å, *V* = 1219.4 (17) Å³, *Z* = 4, *D_x* = 1.340 g cm⁻³, λ(Mo *K*α) = 0.71073 Å, μ = 0.919 cm⁻¹, *F*(000) = 520, *T* = 293 K, *R* = 0.046 for 1291 observations.

Introduction

Flexible molecular structures are often found in crystals to adopt a shape within a range of accessible conformations. The conformation displayed may be thought to result from a complex balance between the energetics of molecular deformation and the crystalline environment. The solid-state structures of many related frozen conformers can in aggregate represent a source of information on the conformations available, and be correlated with solution structure, chemical reactivity (Allen, 1982; Murray-Rust, 1982) or provide pictures of the path of molecular deformation (Bürgi & Dunitz, 1983).

Ring deformation motions are a case in point. Small saturated or partly unsaturated rings are flexible structures. They may not be the most readily crystallizable subjects for ambient temperature study. However, embedded in an appropriate larger molecule and otherwise conformationally unconstrained, small ring motions might well be approximately modelled. The present example consists of the embedded heterocycle 3,4-dihydro-2*H*-pyran (DHP). We have examined DHP in a group of related molecular structures captured in a variety of crystallographic environments. The system consists of 2-hydroxy- and 2-methoxy-2,4-dimethyl-3,4-dihydro-2*H*,5*H*-pyrano[3,2-*c*][1]benzopyran-5-one, hemiketal and methyl ketal derivatives of a compound closely related to the anticoagulant drug, warfarin.



Warfarin	<i>R</i> = C ₆ H ₅	<i>R'</i> = OH	<i>E</i>
(I)	<i>R</i> = CH ₃	<i>R'</i> = OCH ₃	<i>Z</i>
(II <i>a,b</i>)	<i>R</i> = CH ₃	<i>R'</i> = OCH ₃	<i>E</i>
(III)	<i>R</i> = CH ₃	<i>R'</i> = OH	<i>Z</i>

A variety of homologous structures is possible because the parent molecule has two C atoms in asymmetric environments. Thus hemiketals and methyl ketals of racemic and resolved diastereomeric forms occur. Of course, polymorphism and multiple units comprising the primary repeat can be and are encountered. A number of structures have already been studied (Valente, Santarsiero & Schomaker, 1979; Valente & Schomaker, 1984). This contribution contains structures for the resolved *cis*- and *trans*-methyl ketals, (I) and (II), and the resolved *cis*-hemiketal, (III). The *trans*-methyl ketal, (II), contains two molecules [(II*a*) and (II*b*)] in the asymmetric unit. With the four molecular structures described here, the series contains nine observations from six crystal studies. A discussion of the similarities and relationships among the dihydropyrans in all the structures follows.

Experimental

Synthesis

Warfarins are made by the Michael-type addition of unsaturated ketones with 4-hydroxycoumarin (Ikawa, Stahmann & Link, 1944). Using 3-penten-2-one, the racemic hemiketals (2-hydroxy) of the title series were obtained. These derivatives of 4-hydroxycoumarin are weakly acidic and may be resolved through their diastereomeric brucine salts which display slight differential solubilities in 2-propanone. Reaction of the purified hemiketal from the less soluble brucine salt with methanol, in the presence of an acidic catalyst, produced a mixture of resolved diastereomeric methyl ketals. Fractional crystallization from methanol gave the pure diastereomers; large colorless blocks of (I) exhibited trigonal facets with m.p. 407–409 K, and thick colorless plates of (II) had m.p. 414–415 K. Proton NMR spectroscopy showed that (I) is the *cis* and (II) is the *trans* isomer by analogy to the proton NMR spectra for warfarin and its methyl ketals (Valente, Lingafelter, Porter & Trager, 1977) and the related racemic *trans*-methyl ketal (IV) (Valente, Santarsiero & Schomaker, 1979). For (I) [300 MHz, CDCl₃, 294.6 K, δ p.p.m. (reference TMS)]: 1.443, CH₃—CH, d, *J* = 6.9 Hz; 1.655, CH₃—C, s; 1.674, CH_αH_β, dd, *J*_{ax} = 6.6, *J*_{gem} =

14.3 Hz; 2.035, CH_aH_b , dd, $J_{\text{bx}} = 3.2$ Hz; 2.91, methine C— H_x , ddq; 3.36, OCH_3 , s; 7.28, 7.45, 7.81, Ar—H's; for (II): 1.393, CH_3CH , d, $J = 6.6$ Hz; 1.672, CH_3 —C, s; 2.30, CH_aH_b , dd, $J_{\text{ax}} = 11.6$, $J_{\text{gem}} = 14.0$ Hz; 2.674, CH_aH_b , dd, $J_{\text{bx}} = 6.8$ Hz; 3.00, methine C— H_x , ddq; 3.26, OCH_3 , s; 7.27, 7.47, 7.80, Ar—H's. In CDCl_3 solution, the *trans* isomer, (II), has a predominant conformation in which the 2-methoxy group is axial and the 4-methyl group is pseudoequatorial. The *cis* isomer, (I), in solution apparently exists in an equilibrium between conformers in which the 2-methoxy and 4-methyl groups are axial and pseudoaxial or equatorial and pseudo-equatorial, respectively, giving averaged vicinal coupling constants for the *ABM* part of the *ABMX*₃ pattern.

The parent hemiketal (III) in chloroform solution consists of a nearly equal mixture of an intermediate open form and two diastereomeric cyclic hemiketals related to the methyl ketals (I) and (II). The proton NMR spectrum (500 MHz, CDCl_3 , 298 K, δ p.p.m. (reference TMS)) of (III) shows three overlapping spectra; *cis*: 1.44, CH_3 —CH, d, $J = 6.25$ Hz; 1.77, CH_3 —C, s; 2.06, CH_aH_b , dd, $J_{\text{ax}} = 4.6$, $J_{\text{gem}} = 14.0$ Hz; 2.06, CH_aH_b , dd, $J_{\text{bx}} = 6.9$ Hz; 2.97, methine C— H_x , ddq; 3.15, OH, s(br); 7.25, 7.48, 7.78, m's, Ar—H's; *trans*: 1.43, CH_3CH , d, $J = 6.25$ Hz; 1.72, CH_3 —C, s; 1.72, CH_aH_b , dd, $J_{\text{ax}} = 11.25$, $J_{\text{gem}} = 14.0$ Hz; 2.30, CH_aH_b , dd, $J_{\text{bx}} = 7.0$ Hz; 3.05, methine C— H_x , ddq; 3.24, OH, s(br); 7.25, 7.48, 7.77, m's, Ar—H's; open form (unanalyzed): 1.49, CH_3CH , d, $J = 7.3$ Hz; 2.18, CH_3 —C, s; 2.79, CH_aH_b , m; 3.42, methine C— H_x , m; 9.61, OH, s(br); 7.25, 7.48, 7.91, m's, Ar—H's.

It was subsequently observed that when the parent (unresolved) hemiketal is recrystallized from methanol, colorless crystals of (III) are obtained as a conglomerate, individuals being enantiomorphic, m.p. 407–409 K. When the racemic mixture is recrystallized from acetone–water solutions, a crystalline racemic compound (IV) is obtained. If the racemate is first resolved with brucine and recrystallized from acetone–water solutions, an enantiomorphic form (V), distinct from (III), is obtained.

Crystallography

Specimens of (I), $1.0 \times 0.7 \times 0.8$ mm, (II), $0.6 \times 0.6 \times 0.3$ mm, and (III), $0.8 \times 0.4 \times 0.4$ mm, were chosen for data collection on a CAD-4 diffractometer. 25 accurately centered reflections with $30 \leq 2\theta \leq 35^\circ$ were used to determine the cell constants. Intensity data were measured to $2\theta = 60^\circ$ with Mo radiation [$\lambda(K\alpha) = 0.71073$ Å]. For (I), data collection proceeded using the Miller indices for the quadrupally primitive *C*-centered orthogonal cell, h : 0–13, k : 0–23, l : 0–35; while the primitive unit sufficed for

(II), h : 0–13, k : 0–16, l : –17–17, and for (III), h : 0–9, k : 0–18, l : 0–19. The data [3182 for (I), 4354 for (II) and 2040 for (III)] were corrected for Lorentz and polarization effects. Three intensities for each were monitored over the course of the [52.6 h (I), 69.8 h (II), 30.4 h (III)] data collection and showed a linear change of –3.0(10)% for (I), –5.4(28)% for (II), –2.1(74)% for (III); a correction was applied to the data sets for (I) and (II) and their symmetry-equivalent data were averaged [$R_f(\text{I}) = 1.6\%$, $R_f(\text{II}) = 2.2\%$], leaving 2225 (I), 4118 (II) and 2040 (III) unique intensities.

The structures were determined using *MULTAN80* (Main, Fiske, Hull, Lessinger, Germain, Declercq & Woolfson, 1980) and refined using the *SDP* program group (Frenz, 1987). Non-H-atom positions were refined with their isotropic temperature factors by full-matrix least squares minimizing $\sum w(|F_o| - |F_c|)^2$, then with their anisotropic temperature factors. Except for the hydroxy H in (III) which was located in a difference Fourier map, H-atom positions were calculated and placed 1.0 Å from their attached atom. They were assigned *B* values approximately 1.3 times B_{eq} of the adjacent C atom and their positions were adjusted accordingly during refinement of the non-H atoms. Scattering factors were from *International Tables for X-ray Crystallography* (1974, Vol. IV) except for H (Stewart, Davidson & Simpson, 1965). An extinction term of the form proposed by Zachariasen (1963) was introduced in the latter stages of the refinements of (I) and (II). Final agreement factors for (I): $R = 0.040$, $wR = 0.061$, $\text{GOF} = 1.75$ for the 1470 *I* values $\geq 3\sigma_I$, scale = $0.084(2)$, $g = 5.3(15) \times 10^{-7}$; for (II): $R = 0.043$, $wR = 0.058$, $\text{GOF} = 1.62$ for the 2923 *I* values $\geq 3\sigma_I$, scale = $0.094(1)$, $g = 4.9(18) \times 10^{-7}$; and for (III): $R = 0.046$, $wR = 0.059$, $\text{GOF} = 1.655$ for the 1291 *I* values $\geq 3\sigma_I$, scale = $0.0443(1)$. Weights corresponding to $[1/s(I)]$, where $s(I) = [(\sigma I_c)^2 + (0.05F_o^2)]^2$, were used in the refinement on the 173 (I), 343 (II), 204 (III) variables. Final maximum shifts were less than 0.01 times the e.s.d.'s for all variables; maximum difference map excursions were less than +0.17 and –0.16 (I), +0.24 and –0.21 (II), and +0.26 and –0.18 e Å⁻³ (III). Final atom positions and equivalent isotropic vibrational terms for the non-H atoms are given in Tables 1–4.*

Absolute configurations were deduced for (I)–(III) by circular dichroism spectroscopy. Since (I) and (II) were obtained from the less soluble brucine diastereomeric salts of the parent weak acid, and since

* Lists of H-atom positions, anisotropic vibrational amplitudes and structure factors have been deposited with the British Library Document Supply Centre as Supplementary Publication No. SUP 53832 (55 pp.). Copies may be obtained through The Technical Editor, International Union of Crystallography, 5 Abbey Square, Chester CH1 2HU, England.

Table 1. Positions and B_{eq} values for (I)
$$B_{eq} = \frac{1}{3} \sum_i \sum_j B_{ij} a_i^* a_j^* \mathbf{a}_i \cdot \mathbf{a}_j$$

	x	y	z	$B(\text{\AA}^2)$
O1	0.4008 (2)	0.7021 (2)	0.96937 (7)	5.02 (4)
O2	0.1973 (2)	0.4568 (2)	0.95877 (8)	6.56 (5)
O3	0.7198 (2)	0.5840 (2)	0.90245 (6)	4.38 (3)
O4	0.6203 (2)	0.4573 (2)	0.82126 (6)	5.56 (5)
C2	0.3394 (3)	0.5454 (3)	0.9509 (1)	4.65 (5)
C3	0.4476 (2)	0.5027 (2)	0.92597 (8)	3.89 (5)
C4	0.6064 (2)	0.6139 (2)	0.92230 (8)	3.59 (4)
C5	0.8309 (3)	0.8985 (3)	0.9352 (1)	4.56 (6)
C6	0.8780 (3)	1.0530 (3)	0.9537 (1)	5.41 (7)
C7	0.7675 (4)	1.0869 (3)	0.97690 (9)	5.53 (7)
C8	0.6080 (3)	0.9696 (3)	0.9822 (1)	5.08 (6)
C9	0.5614 (3)	0.8167 (2)	0.96358 (8)	4.16 (5)
C10	0.6689 (2)	0.7777 (2)	0.94007 (8)	3.70 (4)
C11	0.3805 (3)	0.3304 (2)	0.90815 (9)	4.37 (5)
C12	0.5209 (3)	0.2978 (3)	0.8986 (1)	5.07 (6)
C13	0.6662 (3)	0.4341 (3)	0.8726 (1)	4.75 (5)
C14	0.8108 (3)	0.4109 (3)	0.8738 (2)	6.74 (7)
C15	0.2662 (3)	0.8265 (3)	0.8596 (1)	5.78 (7)
C16	0.7469 (3)	0.5833 (3)	0.7894 (1)	6.59 (8)

Table 4. Positions and B_{eq} values for (III)
$$B_{eq} = \frac{1}{3} \sum_i \sum_j B_{ij} a_i^* a_j^* \mathbf{a}_i \cdot \mathbf{a}_j$$

	x	y	z	$B(\text{\AA}^2)$
O1	0.0607 (3)	0.7713 (1)	0.6802 (1)	3.42 (4)
O2	0.0494 (4)	0.8961 (2)	0.7881 (1)	4.55 (5)
O3	0.0492 (3)	0.9815 (1)	0.4578 (1)	3.34 (4)
O4	0.2723 (3)	1.1160 (1)	0.4747 (1)	3.94 (4)
C2	0.0548 (5)	0.8757 (2)	0.7028 (2)	3.22 (5)
C3	0.0553 (5)	0.9505 (5)	0.6269 (2)	2.91 (5)
C4	0.0549 (4)	0.9181 (2)	0.5339 (2)	2.53 (4)
C5	0.0542 (4)	0.7694 (2)	0.4171 (2)	2.95 (5)
C6	0.0557 (5)	0.6634 (2)	0.4011 (2)	3.51 (5)
C7	0.0578 (5)	0.5951 (2)	0.4784 (2)	3.51 (5)
C8	0.0590 (5)	0.6310 (2)	0.5712 (2)	3.47 (5)
C9	0.0584 (4)	0.7375 (2)	0.5864 (2)	2.75 (5)
C10	0.0551 (4)	0.8085 (2)	0.5111 (2)	2.52 (4)
C11	0.0490 (5)	1.0643 (2)	0.6531 (2)	3.60 (6)
C12	-0.0210 (5)	1.1266 (2)	0.5664 (2)	4.16 (7)
C13	0.0719 (5)	1.0951 (2)	0.4723 (2)	3.61 (6)
C14	-0.0271 (7)	1.1415 (3)	0.3856 (2)	5.74 (9)
C15	0.2453 (6)	1.1002 (2)	0.6949 (2)	4.47 (7)

Table 2. Positions and B_{eq} values for (IIa)
$$B_{eq} = \frac{1}{3} \sum_i \sum_j B_{ij} a_i^* a_j^* \mathbf{a}_i \cdot \mathbf{a}_j$$

	x	y	z	$B(\text{\AA}^2)$
O1A	0.8954 (2)	0.620	0.2901 (1)	4.64 (4)
O2A	1.1345 (2)	0.6580 (2)	0.3596 (2)	6.47 (5)
O3A	0.7839 (2)	0.7499 (2)	0.5552 (1)	4.20 (3)
O4A	0.9654 (2)	0.6759 (2)	0.7033 (1)	4.64 (4)
C2A	1.0101 (3)	0.6675 (3)	0.3713 (2)	4.32 (5)
C3A	0.9729 (2)	0.7211 (2)	0.4622 (2)	3.71 (4)
C4A	0.8298 (2)	0.7125 (2)	0.4700 (2)	3.37 (4)
C5A	0.5632 (3)	0.6501 (2)	0.3905 (2)	4.00 (5)
C6A	0.4579 (3)	0.5970 (3)	0.3084 (2)	4.56 (6)
C7A	0.5012 (3)	0.5510 (3)	0.2206 (2)	5.02 (6)
C8A	0.6456 (3)	0.5589 (3)	0.2152 (2)	4.75 (6)
C9A	0.7503 (3)	0.6147 (2)	0.2971 (2)	3.85 (5)
C10A	0.7122 (2)	0.6596 (2)	0.3870 (2)	3.34 (4)
C11A	1.0956 (3)	0.7787 (3)	0.5494 (2)	4.51 (5)
C12A	1.0243 (3)	0.8413 (2)	0.6269 (2)	4.89 (6)
C13A	0.9013 (3)	0.7770 (2)	0.6554 (2)	4.30 (5)
C14A	0.8190 (4)	0.8416 (3)	0.7232 (2)	6.05 (7)
C15A	1.1914 (4)	0.8589 (3)	0.5041 (3)	7.64 (9)
C16A	0.8664 (4)	0.5966 (3)	0.7292 (2)	5.88 (7)

Table 3. Positions and B_{eq} values for (IIb)
$$B_{eq} = \frac{1}{3} \sum_i \sum_j B_{ij} a_i^* a_j^* \mathbf{a}_i \cdot \mathbf{a}_j$$

	x	y	z	$B(\text{\AA}^2)$
O1B	0.7434 (2)	0.9240 (2)	0.1545 (1)	4.74 (4)
O2B	0.7442 (2)	0.8847 (3)	-0.0137 (2)	6.27 (5)
O3B	0.3151 (2)	0.8071 (2)	0.1063 (1)	4.08 (3)
O4B	0.1872 (2)	0.8767 (2)	-0.0637 (1)	4.25 (3)
C2B	0.6759 (3)	0.8775 (2)	0.0538 (2)	4.29 (5)
C3B	0.5292 (2)	0.8271 (2)	0.0374 (2)	3.48 (4)
C4B	0.4566 (2)	0.8402 (2)	0.1161 (2)	3.21 (4)
C5B	0.4563 (3)	0.9073 (2)	0.3021 (2)	4.22 (5)
C6B	0.5299 (3)	0.9602 (3)	0.3979 (2)	5.25 (6)
C7B	0.6739 (4)	0.9990 (3)	0.4117 (2)	5.70 (7)
C8B	0.7459 (3)	0.9868 (3)	0.3309 (2)	5.23 (6)
C9B	0.6712 (2)	0.9328 (2)	0.2347 (2)	3.91 (5)
C10B	0.5266 (2)	0.8938 (2)	0.2191 (2)	3.42 (4)
C11B	0.4580 (3)	0.7663 (2)	-0.0679 (2)	4.20 (5)
C12B	0.3155 (3)	0.7086 (2)	-0.0592 (2)	4.59 (5)
C13B	0.2237 (3)	0.7781 (2)	-0.0026 (2)	4.08 (5)
C14B	0.0896 (3)	0.7171 (3)	0.0177 (3)	6.05 (7)
C15B	0.5629 (4)	0.6805 (3)	-0.0976 (3)	6.52 (7)
C16B	0.1095 (3)	0.9614 (3)	-0.0222 (2)	5.54 (6)

the hemiketal from the more soluble salt had been assigned the 4R configuration (Valente & Schomaker, 1984) on the basis of its similarity to warfarin (Valente & Trager, 1978), the 4S configuration seemed likely. In fact, circular dichroism spectra of the data crystals of (I) and (II) dissolved in methanol showed large negative Cotton effects near 220 nm, confirming the 4S assignment. (I) is the 2S,4S isomer and (IIa,b) are 2R,4S isomers. The space-group enantiomorph for (I) is therefore established. The circular dichroism spectrum of the data crystal for (III), which was selected from a conglomerate, showed a large negative Cotton effect near 220 nm also. Thus its constituent molecules happened to have the 2S,4S configuration.

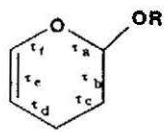
Principal-component analysis

To search for the likely interrelation between torsional variances within the dihydropyran rings of structures (I)–(VI), a factor analysis was performed on the torsion angles. Values for these angles taken from Table 5 were converted to radians and normalized ($\tau' = \tau\pi/180$) by the mean length of the dihedral arms. For a data matrix, **A**, with nine rows (molecules) and six columns (normalized torsions), a 6×6 correlation matrix **B** is defined by $\mathbf{B} = 1/(a-1)\mathbf{A}^T\mathbf{A}$. Significantly nonzero eigenvalues of **B** represent the principal components. Programs used were those contained in the SPSS package (Norris, 1986). Factors and the correlations of the torsion variables with the principal components are given in Table 6. A single large eigenvalue could be extracted which accounted for 75% of the sample variance.

Results and discussion

Ellipsoid plots (Johnson, 1976) of the molecular structures of (I), (IIa), (IIb) and (III) are given in

Table 5. Selected dihydropyran ring features



	Torsion angles (°)*						Displacement asymmetry values†	
	τ_a	τ_b	τ_c	τ_d	τ_e	τ_f	ΔC_2	ϕ
(I)	-39.7	53.3	-39.3	12.6	0.4	13.6	-0.005	91.9
(IIa)	-44.0	58.2	-41.4	11.4	2.2	14.8	-0.007	91.2
(IIb)	-43.6	57.9	-40.7	10.2	3.8	14.0	-0.008	91.6
(III)	-34.3	52.9	-44.1	17.6	0.1	8.8	0.041	77.0
(IV)	-48.4	60.4	-39.0	6.8	5.0	16.9	-0.034	98.2
(Va)	-37.5	59.3	-49.3	20.9	1.0	7.6	0.059	73.3
(Vb)	-37.9	54.8	-45.2	18.3	2.2	12.4	0.031	80.4
(VIa)	-35.5	53.4	-43.3	16.8	-0.9	9.8	0.034	78.9
(VIb)	-35.8	54.1	-43.5	16.2	1.3	8.9	0.034	79.2

* E.s.d.'s about 0.3°; for (V), 1.0°; employing a common configuration.

† Nardelli (1983).

Table 6. Results of principal-component (factor) analysis

	Factor 1	Factor 2*
Eigenvalue (variance)	4.488 (75%)	1.216 (20%)
Factor matrix†		
τ_a	-0.980	-0.158
τ_c	0.753	-0.649
τ_d	-0.946	0.278
τ_e	0.867	0.353
τ_f	0.941	-0.198
τ_b	0.655	0.728

* Additional eigenvalues: 0.174, 0.119, 0.002, 0.000.

† Strong correlations are given in bold type.

Figs. 1-4. In each, the 2-methoxy or 2-hydroxy group is disposed axially on the DHP ring which is fused with the benzopyran moiety. This arrangement is the more stable anomeric configuration in which the 4-methyl substituent (at C15) is disposed pseudoaxially in (I) and (III) and pseudoequatorially in (IIa,b), respectively *cis* and *trans* to the 2-methoxy(hydroxy) group. Ketal methyls in (I) and (IIa,b) and the hydroxy H in the hemiketal (III) orient *exo* to the ring and *gauche* to the endocyclic C_{sp^3} -O bond, the more stable exoanomeric conformation. Bond lengths and angles have normal values; all three structures show the somewhat elongated dihydropyranyl C_{sp^3} -O bond [1.464 (2) Å in (I); 1.469 (3), 1.456 (2) Å in (IIa,b); 1.479 (3) Å in (III)] common in these structures (Valente, Santarsiero & Schomaker, 1979). Average and maximal differences for bond lengths and angles between the two *trans* structures (IIa,b) are 0.007, 0.024 Å and 0.4, 1.2°, suggesting that the e.s.d.'s of the derived values are underestimated perhaps by a factor of two. A comparison between *trans* (IIa,b) (mean) and the *cis*-methyl ketal structure (I) gives 0.008, 0.025 Å and

0.8, 3.8°; lengths between the isomers agree at about 3σ but angles agree less well especially in structural aspects in which the molecules differ configurationally. Torsion comparisons are less instructive since the flexible DHP ring features are sensitive not only to configuration but also to the molecular environments in the differing crystals. Molecules in structures (I) and (II) pack without unusual close contacts. In (III), hydroxyls are intermolecularly hydrogen bonded to coumarin carbonyl groups between molecules related by the screw axis along *c*. The distance between O atoms in the hydrogen bond is O(4)⋯O(2) = 2.877 (2) Å; the angle subtended at H is 167°.

Chemical relationships among the various structures (I)-(VI) are given in Fig. 5. Five of the nine

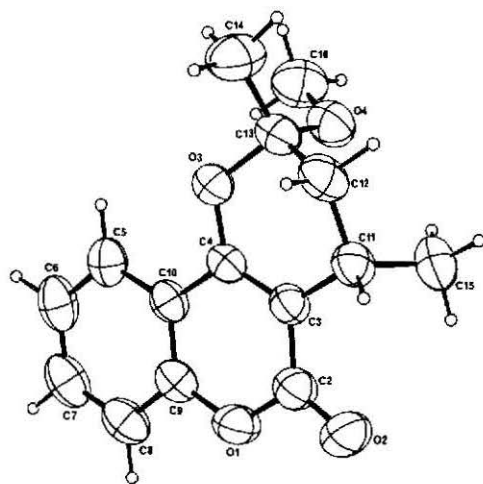


Fig. 1. An ORTEP (Johnson, 1976) plot of the molecular structure of (I) with probability vibrational ellipsoids for the non-H atoms.

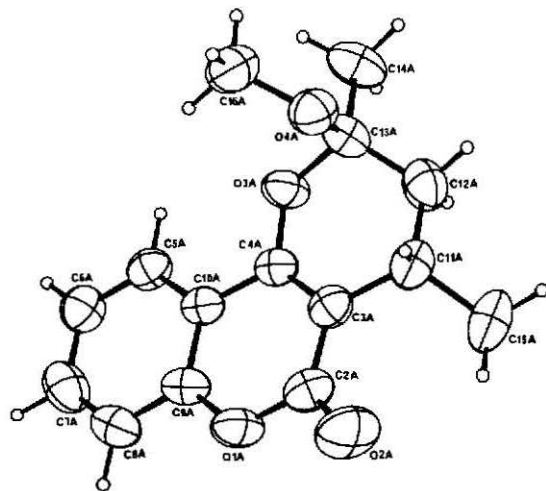


Fig. 2. A plot of the structure of (IIa).

structures are hemiketals. Four of these occur with *cis* configuration (2-hydroxy to 4-methyl) and one with *trans*. In each, the 2-O atom substituent is in the more stable axial anomeric form. Magnetic resonance studies show a dynamic equilibrium between the configurational isomers and an intermediate open form, each of which is about equally abundant in solution (Valente, Santarsiero & Schomaker, 1979). Crystallization seems slightly to favor formation of *cis* hemiketals, though the observation of one *trans* isomer at least qualitatively accords with the solution importance of this isomer.

Some physical information on the crystalline forms (I)–(VI) is given in Table 7 along with that for two other phases (*A*, *B*) for which structures are not known. Hemiketal crystals have generally higher melting temperatures and densities than the methyl ketals. All hemiketals are involved in intermolecular hydrogen bonding in the crystals. A somewhat larger decrease in molecular volume than that necessary to

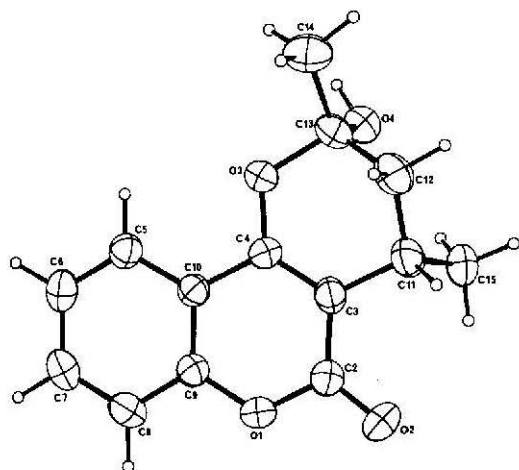


Fig. 3. A plot of the structure of (IIb).

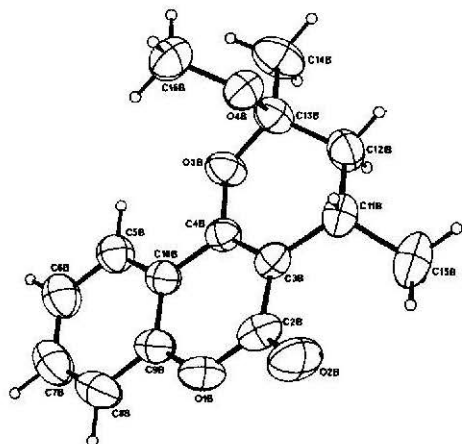


Fig. 4. A plot of the structure of (III).

Table 7. Selected physical properties of the phases within the series

	M.p. (K)	D_s (g cm ⁻³)	V /molecule (Å ³)	Type*
(I)	385	1.31	330	M†
(IIa,b)	405	1.27	339	M†
(III)	408	1.34	305	H†
(IV)	394	1.31	331	M
(Va,b)	404	1.32	308	H†
(VIa,b)	414	1.35	302	H
<i>A</i>	Oil	—	—	M
<i>B</i>	424	—	—	H†

* M – methyl ketal, $M_r = 322$; H – hemiketal, $M_r = 308$.

† Resolved.

accompany the lower mass in hemiketals compared to the methyl ketals implies a slightly more efficient packing in the former.

A comparison of the conformations of the DHP's in (I), (IIa,b) and (III) is more useful when included within the group of nine related structures. Embedded DHP's are actually 2-hydroxy and 2-methoxydihydropyranyl (hemi)ketals whose rings are near the center of the molecule. Typically the otherwise unsubstituted methylene C12 has the largest vibrational amplitude of the ring atoms, while others have amplitudes at or below the mean for all the non-H atoms. Derived structural features have not been corrected for small vibrationally related effects. The shape of the DHP ring is approximately related to that of cyclohexene which in the ground state has a half-chair C_2 conformation, and the intraring torsion angle at the unsaturation, τ_e , is zero. Interconversion between equivalent half-chair forms can occur through distortion of the ground-state form along either of two identical paths initially through

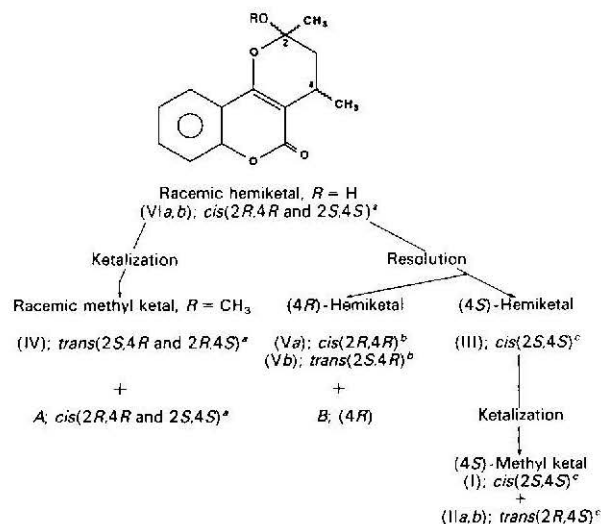
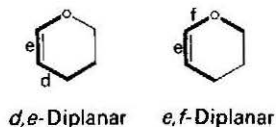
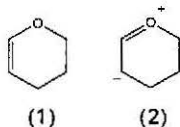


Fig. 5. Relationships between structural homologs containing the embedded dihydropyran ring: (a) Valente, Santarsiero & Schomaker (1979); (b) Valente & Schomaker (1984); (c) this work.

the 1,2-diplanar sofa forms (Rabideau, 1989). DHP is similarly deformable in its half-chair interconversion but lacking the symmetry of cyclohexene, the pseudorotation occurs along inequivalent paths. Two sofa conformations are distinguishable, *d,e*- and *e,f*-diplanar forms, so named for the adjacent endocyclic ring bonds with small torsion angles. Such deviations from idealized symmetry can be used to assess the extent and direction of ring distortions through the displacement asymmetry parameters described by Nardelli (1983). Table 5 presents these and the intraring torsion angles for the DHP rings in structures (I)–(VI).



All of the DHP structures are nearly half-chairs as seen by the relatively small ΔC_2 values. The mean ring structure may be described as a half-chair slightly distorted towards the *e,f*-diplanar form ($\Delta C_2 = 0.016$). Such a structure is not unlike that determined from microwave data on gaseous dihydropyran (López & Alonso, 1985), or implied from magnetic resonance data (Bushweller & O'Neil, 1969) on pure liquid dihydropyran at ambient temperature. Compared with saturated cyclic ethers, the shorter C_{sp^2} —O bond (1.35 Å) and widened intraring angle at O ($\approx 116^\circ$) suggest contributions to the ground-state structure (1) by resonance structures like (2) which arise as a consequence of charge delocalization within enol ethers.



In the nine embedded DHP structures, a range of conformations is observed. Deviations from the mean are significant in that the methyl ketals are distorted more towards the *d,e*-diplanar form ($-\Delta C_2$ values) and the hemiketals more towards the *e,f*-diplanar form ($+\Delta C_2$ values). A similar trend can be found in a comparison of analogous warfarin hemiketals and methyl ketals. The 2-methoxy group appears to distort the DHP ring from the near C_2 shape preferentially along the path in the direction of the *d,e*-diplanar form. Since the DHP ring is easily deformable, even the relatively minor substitution of a methyl for a H atom on the 2-O atom apparently shifts the equilibrium conformation of the DHP ring as deduced from the mean in the group of structures comprising the sample. The range of accessible DHP ring conformations in the methyl ketals complements

those seen in the hemiketals. While these distributions are probably not accidental, the nine structures in the present group are representative of modestly distorted DHP rings.

The range of values for the intraring torsions in the structures generally accords with expectations about the rigidity of the ring. Torsion τ_e displays the least flexibility but shows a tendency to twist in concert with the adjacent torsion involving the ring O atom (τ_f). In conformers distorted more toward the *d,e*-diplanar forms, τ_e increases and absorbs some of the twist strain together with τ_f . The effect is not evident in the DHP's distorted toward the *e,f*-diplanar forms, in which τ_e remains nearly untwisted or seems to reach a minimum as τ_d begins to increase. Consequently the range of τ_f is about two-thirds that of τ_d among the structures, suggesting a slightly stiffer torsional barrier about τ_f which is consistent with the resonance contribution of structure (2) described above.

Among the remaining torsions, τ_a and τ_c vary inversely over about the same range, in agreement with calculations on cyclohexene (Bucourt, 1974). Torsion τ_b is expected to reach a maximum of about 60° in the vicinity of the ground-state form. In the present group, τ_b weakly correlates with ring distortion, but its range and scatter make rationalization uncertain. A line drawing of several distinct conformations superposed is given in Fig. 6 from a perspective viewing through the ring approximately normal to the ring plane and towards the double bond. A ring bending model can be inferred as a motion of the O— C_{sp^2} — C_{sp^2} —C atoms with respect to the more rigid enol ether backbone of the ring.

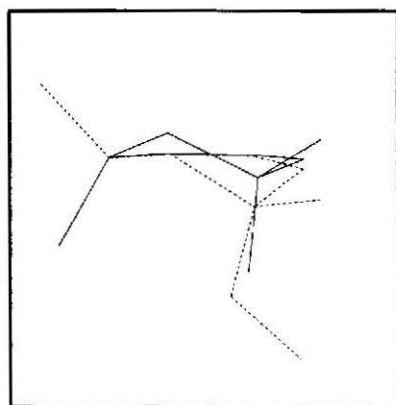


Fig. 6. A perspective composite line drawing connecting atoms in the dihydropyran rings having differing conformations. The view is through the ring towards the double bond, and approximately normal to the mean ring plane. DHP rings from (I), (IV) and (VIa) in Table 5 are shown and illustrate both the half-chair and *d,e*-diplanar forms observed in this series. The orientation is looking into the C(3)—C(4) double bond with O(4) on the right.

The extent of the dihydropyran ring deformation modelled in the structures embraces only a very modest range near the expected lowest energy conformer. Current views acknowledge the unlikelihood that conformations with energies greater than 0.84 kJ mol⁻¹ per parameter above the ground state can be stabilized by the crystalline environs (Murray-Rust, 1982). Thus, for an entire structure, perhaps a realistic upper limit is 8.4–12.6 kJ mol⁻¹. For DHP, Raman and infrared spectroscopic work has established that the principal low-energy excitations involve ring bending and single-bond twisting modes (Durig, Carter & Carreira, 1974; Lord, Rounds & Ueda, 1972). Extrapolations of these provided a model for the higher energy conformers on the path of pseudorotation and a calculation of the barrier height. From a recent reanalysis of the vibrational energy surface for DHP (Tecklenburg & Laane, 1989), it was concluded that the model for the interconversion of DHP is improved by inclusion of the double-bond twisting vibrational mode. The conformations of the DHP's found in crystal structures are less than about 4.2 kJ mol⁻¹ from the lowest energy form having a near C₂ structure [as deduced by molecular-mechanics methods following the treatment of Dodziuk, von Vothenberg & Allinger (1982)], and the motions of the heterocycle implied by the structures are principally a bending of the two aliphatic out-of-plane atoms with respect to the stiffer C=C—O backbone. Bending brings the C_{sp³} adjacent to O nearer the plane described by the backbone diminishing τ_f and leads to the *e,f*-diplanar form; alternatively, bending away from it increases τ_f and to a lesser extent τ_e in complicity, and leads to the *d,e*-diplanar conformation. Crystal structures show that double-bond twisting is important in the path of pseudorotation of DHP even when the extent of deformations and their energies are small.

When factor analysis is applied to the torsional variance within the group of nine structures, a similar model for the DHP deformation emerges. Using the six intraring (normalized) torsions, factor analysis reveals a single ring distortion feature which accounts for three-quarters of the sample variance (Table 6). This factor reveals the necessarily strongly concerted changes in all intraring torsions, probably excepting τ_b , and may be understood in terms of a ring bending and double-bond twisting motion. While τ_a and τ_d decrease and τ_e increases, the distortion towards the *d,e*-diplanar form involves an increase in both τ_e and τ_f . These changes are of the type described for interconversion of cyclohexene (Bucourt, 1974) based on molecular mechanics. The second highest factor has an eigenvalue too small to account for more than the nominal variance in any variable, so it probably represents mostly random errors.

Examination of several embedded dihydropyran rings bearing 4-methyl substituents reveals an ensemble of ring conformations which includes half-chair forms near the expected lowest energy conformer as well as forms distorted toward either of the two sofa forms. Even such modestly distorted rings as discussed here are characterized by double-bond twisting, suggesting that this vibrational mode is indeed an important one in considerations of the vibrational energy surface for DHP. Overall, intraring torsions, with the exception of τ_b , exhibit strongly concerted changes. Greater distortions of the dihydropyran ring can be stabilized in warfarin analogs with somewhat larger 4-substituents (Valente, Eggleston & Schomaker, 1987). In these, evidence for both ring bending, single-bond and double-bond twisting can be seen. These results along with a molecular-mechanical model will be presented in the future.

We extend our thanks to Mr John Burgardt, Mississippi College, for experimental help and to Dr Eric Noe, Jackson State University, for NMR measurements. We gratefully acknowledge support under grant MS-86-G-10 from the Mississippi Affiliate of the American Heart Association.

References

- ALLEN, F. H. (1982). *Molecular Structure and Biological Activity*, edited by J. F. GRIFFIN & W. L. DUAX, pp. 105–116. New York: Elsevier Biomedical.
- BUCOURT, R. (1974). *Top. Stereochem.* **8**, 183–187.
- BÜRGI, H.-B. & DUNITZ, J. D. (1983). *Acc. Chem. Res.* **16**, 153–161.
- BUSHWELLER, C. H. & O'NEIL, J. W. (1969). *Tetrahedron Lett.* **53**, 4713–4716.
- DODZIUK, H., VON VOTHENBERG, H. & ALLINGER, N. L. (1982). *Tetrahedron*, **38**, 2811–2819.
- DURIG, J. R., CARTER, R. O. & CARREIRA, L. A. (1974). *J. Chem. Phys.* **60**, 3098–3101.
- FRENZ, B. A. (1987). *Structure Determination Package*. Enraf-Nonius, Delft, The Netherlands.
- IKAWA, M., STAHMANN, M. & LINK, K. P. (1944). *J. Am. Chem. Soc.* **66**, 902–906.
- JOHNSON, C. K. (1976). *ORTEPII*. Report ORNL-5138. Oak Ridge National Laboratory, Tennessee, USA.
- LÓPEZ, J. C. & ALONSO, J. L. (1985). *Z. Naturforsch. Teil A*, **40**, 913–919.
- LORD, R. C., ROUNDS, R. C. & UEDA, T. (1972). *J. Chem. Phys.* **57**, 2572–2580.
- MAIN, P., FISKE, S. J., HULL, S. E., LESSINGER, L., GERMAIN, G., DECLERCQ, J.-P. & WOOLFSON, M. M. (1980). *MULTAN80. A System of Computer Programs for the Automatic Solution of Crystal Structures from X-ray Diffraction Data*. Univs. of York, England, and Louvain, Belgium.
- MURRAY-RUST, P. (1982). *Molecular Structure and Biological Activity*, edited by J. F. GRIFFIN & W. L. DUAX, pp. 117–131. Amsterdam: Elsevier.
- NARDELLI, M. (1983). *Acta Cryst.* **C39**, 1141–1142.
- NORUSIS, M. J. (1986). *Statistical Package for the Social Sciences*. SPSS Inc., Chicago, IL, USA.

- RABIDEAU, P. W. (1989). Editor. *The Conformational Analysis of Cyclohexenes, Cyclohexadienes, and Related Hydroaromatic Compounds*. New York: VCH Publishers.
- STEWART, R. F., DAVIDSON, E. R. & SIMPSON, W. T. (1965). *J. Chem. Phys.* **42**, 3176-3187.
- TECKLENBURG, M. J. & LAANE, J. (1989). *J. Am. Chem. Soc.* **111**, 6920-6926.
- VALENTE, E. J., EGGLESTON, D. S. & SCHOMAKER, V. (1987). *Acta Cryst.* **C43**, 533-536.
- VALENTE, E. J., LINGAFELTER, E. C., PORTER, W. R. & TRAGER, W. F. (1977). *J. Med. Chem.* **20**, 1489-1493.
- VALENTE, E. J., SANTARSIERO, B. D. & SCHOMAKER, V. (1979). *J. Org. Chem.* **44**, 798-802.
- VALENTE, E. J. & SCHOMAKER, V. (1984). *Acta Cryst.* **C40**, 1068-1070.
- VALENTE, E. J. & TRAGER, W. F. (1978). *J. Med. Chem.* **21**, 141-143.
- ZACHARIASEN, W. H. (1963). *Acta Cryst.* **16**, 1139-1144.